ACS Combinatorial Science

pubs.acs.org/acscombsci

Letter

Use of Target-Displaying Magnetized Yeast in Screening mRNA-Display Peptide Libraries to Identify Ligands

Kaitlyn Bacon,[§] John Bowen,[§] Hannah Reese, Balaji M. Rao,* and Stefano Menegatti*

Cite This: *ACS Comb. Sci.* 2020, 22, 738−744

Read Online

ACCESS | Metrics & More | Article Recommendations | Supporting Information

ABSTRACT: This work presents the first use of yeast-displayed protein targets for screening mRNA-display libraries of cyclic and linear peptides. The WW domains of Yes-Associated Protein 1 (WW-YAP) and mitochondrial import receptor subunit TOM22 were adopted as protein targets. Yeast cells displaying WW-YAP or TOM22 were magnetized with iron oxide nanoparticles to enable the isolation of target-binding mRNA-peptide fusions. Equilibrium adsorption studies were conducted to estimate the binding affinity (K_D) of select WW-YAP-binding peptides: K_D values of 37 and 4 μM were obtained for cyclo[M-AFRLC-K] and its linear cognate, and 40 and 3 μM for cyclo[M-LDFVNHRSRG-K] and its linear cognate, respectively. TOM22-binding peptide cyclo[M-PELN-RAI-K] was conjugated to magnetic beads and incubated with yeast cells expressing TOM22 and luciferase. A luciferase-based assay showed a 4.5-fold higher binding of TOM22$^+$ yeast compared to control cells. This work demonstrates that integrating mRNA- and yeast-display accelerates the discovery of peptide ligands.

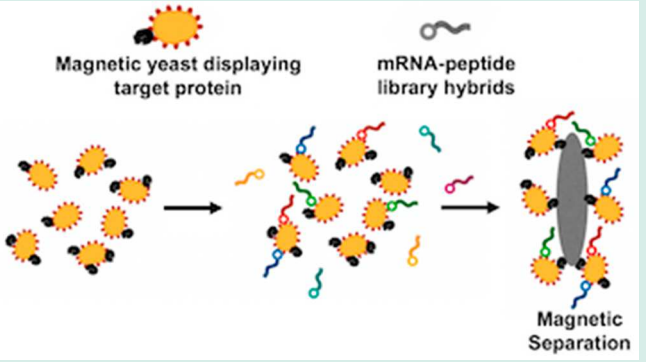

KEYWORDS: *yeast surface display, yeast magnetization, peptide ligands, mRNA-display library, ligand discovery*

Cell-free combinatorial libraries, such as ribosomal- and mRNA-display, are attractive tools in ligand discovery owing to their chemical diversity and ease of post-translational modifications.[1] In the mRNA-display platform, a peptide sequence is connected to its coding mRNA via a puromycin linkage.[2] The mRNA is reverse transcribed to form mRNA-cDNA-peptide fusions that can be used in library screening to identify peptide affinity ligands. Following library selection, the DNA linked to the peptide fusions that bind the target is amplified and sequenced. This technology is widely utilized in the discovery of short peptides,[3] which are of great interest for use as tags or modulators of protein−protein interactions;[4] short peptides are also amenable to post-translational modifications, such as cyclization, which typically imparts higher target binding affinity and proteolysis resistance.[5] In prior work, our group developed a method to generate mRNA-display libraries of cyclic peptides via head-to-side chain chemical cross-linking of peptide-mRNA fusions adsorbed on a solid phase.[6]

The selection of mRNA-display peptide libraries is commonly performed against a target protein conjugated onto synthetic magnetic nanoparticles.[6] Generally, recombinant expression and subsequent purification is required to obtain a soluble form of the target protein to be immobilized. As an alternative, the target protein can be expressed as a yeast cell surface fusion using the yeast surface display platform.[7] The use of yeast-displayed targets is particularly impactful for proteins that require a eukaryotic host for appropriate expression.[8] Yeast-displayed targets have been employed to identify binding proteins specific to membrane protein targets from both phage- and yeast-display libraries.[7,9] However, their use in screening mRNA-display libraries has not been previously explored.

The use of yeast-displayed targets for screening mRNA-display libraries poses a challenge: how to separate the selected fusions from the unbound portion of the library. As the fusions are soluble, the use of centrifugation for separating yeast-bound fusions represents an option; however, removal of the unbound fusions is tedious. Unbound fusions from even small amounts of residual liquid may lead to a significant fraction of false positives. This highlights the need for improved isolation techniques capable of reducing carryover and increasing selection stringency.

To address this challenge, this work presents the use of magnetized yeast cells as protein-display particles to increase the efficiency of isolating lead mRNA-peptide fusions (Figure 1). Yeast are magnetized by adsorbing iron oxide nanoparticles (IONs) onto anionic moieties that constellate on the cell wall

Received: August 12, 2020
Revised: October 7, 2020
Published: October 22, 2020

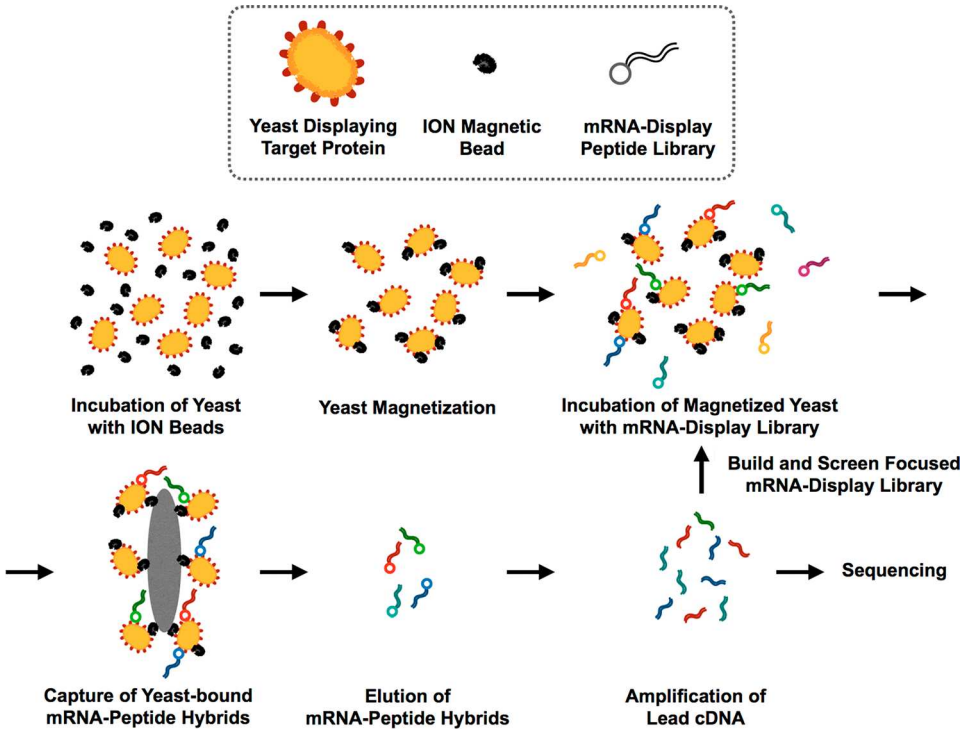

Figure 1. Non-specific yeast cell magnetization and mRNA-display peptide library screening against magnetic yeast targets. Yeast cells expressing WW-YAP or TOM22 were incubated with iron oxide magnetic nanoparticles (ION magnetic beads). Magnetic yeast cells were separated from non-magnetized yeast cells using a magnet. The mRNA-display peptide library was then incubated with the magnetized target cells. Any mRNA-display peptide fusions bound to the target cells were isolated using a magnet. After, the positively bound mRNA-display peptide fusions were eluted from the target cells. DNA linked to the eluted clones was amplified, and a new library was synthesized using this DNA as the template for the next round of screening. Additional rounds of selection against the target cells were performed. The stringency of elution increased for each selection round.

in a pH-controlled environment.[10] Yeast expressing proteins with varying isoelectric points can be magnetized by adjusting the pH of the buffer in which the IONs are adsorbed.[11] Following adsorption, the IONs are blocked with albumin to prevent non-specific adsorption of mRNA-peptide hybrids and other species in solution. The selection of mRNA-display libraries generally takes place at a pH of 7.4. If yeast cells are magnetized at a different pH, IONs can dissociate when the magnetic yeast cells are incubated in the selection buffer. mRNA-peptide hybrids associated with a demagnetized yeast cell are subsequently lost. Nonetheless, more than 50% of non-specifically magnetized cells maintain their magnetized state over the course of a selection.[7] As an alternative, affinity-based magnetization methods can be used, which result in lower losses due to target cell de-magnetization (~30% loss).[7] The size of mRNA-display libraries (~10^{12} hybrids, corresponding to ~1000 copies per peptide in case of 7-mers) and the number of target proteins expressed on yeast (~50 000 per cell[12,13]) ensure ample contact between the library and the target proteins. Also, because there are multiple copies of each peptide in the library, it is likely that any peptide with affinity for the target will be isolated even if some fusions are lost due to ION desorption.

In this work, a combinatorial library of cyclic peptides generated using mRNA-display was screened against magnetized target yeast to identify peptides with affinity for the tandem WW domain of Yes-Associated Protein 1 (WW-YAP) and mitochondrial surface protein TOM22. YAP is an effector protein of the Hippo Signaling pathway regulating cellular amplification and survival,[14] while TOM22 is a mitochondrial membrane protein involved in the recognition and translocation of mitochondrial pre-proteins produced in the cytosol.[15] Peptides capable of inhibiting the binding of cytoplasmic proteins to the WW domains of YAP can provide mechanistic insight into the Hippo-YAP pathway and a means to regulate cell proliferation. Peptides with affinity for TOM22 have the potential be used for targeted delivery of therapeutic payloads to treat patients with mitochondrial deficiencies.[16] WW-YAP and TOM22 were expressed on the surface of EBY100 yeast using the yeast surface display platform (surface display levels detailed in Figure S1).[17] The cells were magnetized with IONs and utilized as targets during subsequent selections of mRNA-display peptide libraries.

A mRNA-display library of cyclic peptides was constructed using a previously developed method of head-to-side chain cyclization that employs a glutarate linker to tether amine groups within methionine and lysine residues flanking the variable peptide segment (NNN degeneracy).[6,18] Prior to selecting against target yeast cells, the library was negatively screened against magnetized yeast displaying a non-target protein (i.e., Fc portion of human IgG, hFc) to remove fusions bound to non-specific, yeast surface proteins. Throughout the library selection process, the stringency of the elution conditions was increased to promote isolation of high-affinity binders. Initially, the mRNA-peptide fusions were eluted from the target cells using 0.15 M potassium hydroxide; in later rounds, the yeast-bound peptides were washed with a mild acidic buffer (50 mM NaCl in 50 mM sodium acetate at pH 5) prior to alkaline elution to remove weakly bound peptides and increase the probability of isolating true affinity binders.

https://dx.doi.org/10.1021/acscombsci.0c00171
ACS Comb. Sci. 2020, 22, 738−744

A)

	M	X_1	X_2	X_3	X_4	X_5	X_6	X_7	X_8	X_9	X_{10}	K
WW.1		A	F	R	L	C						
WW.2		R	L	I	M	G						
WW.3		S	P	A	G	L						
WW.4		T	L	V	I	R	L	G				
WW.5		E	M	E	R	I	S	C				
WW.6		Y	R	G	D	P	E	T	C	V	D	
WW.7		T	P	E	S	V	X	R	S	S	I	
WW.8		D	G	N	L	S	G	I	M	P	V	
WW.9		S	L	L	T	R	V	L	Q	G	X	
WW.10		L	D	F	V	N	H	R	S	R	G	

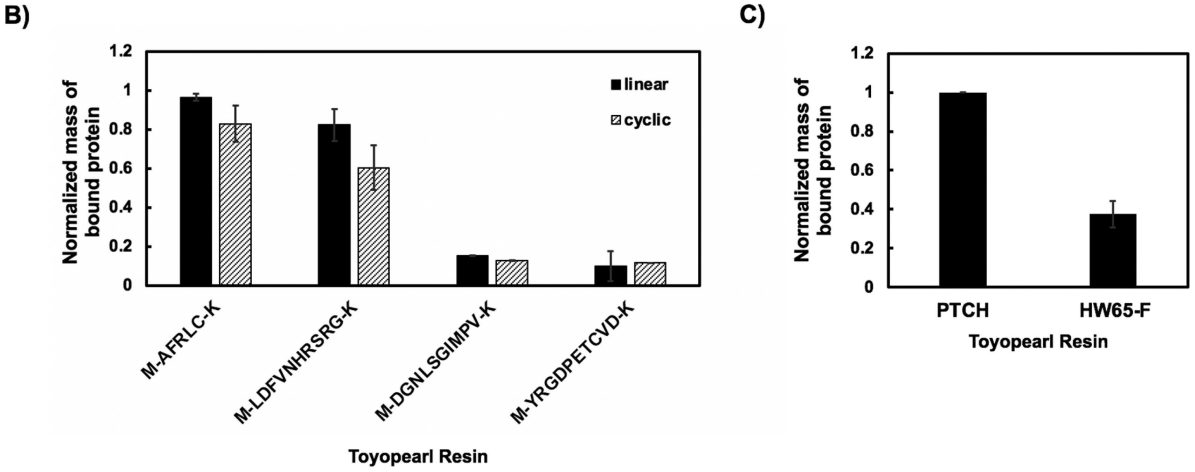

Figure 2. Identified WW-YAP-binding cyclic peptides and primary evaluation of lead candidates. (A) Amino acid sequences of peptides isolated from the selection of a mRNA-display cyclic peptide library against yeast cells displaying WW-YAP. (B) Soluble WW-YAP protein (1 mg/mL) was incubated with cyclo[M-AFRLC-K]-Toyopearl, MAFRLCK-Toyopearl, cyclo[M-LDFVNHRSRG-K]-Toyopearl, MLDFVNHRSRGK-Toyopearl, cyclo[M-DGNLSGIMPV-K]-Toyopearl, MDGNLSGIMPVK-Toyopearl, cyclo[M-YRGDPETCVD-K]-Toyopearl, and MYRGDPETCVDK-Toyopearl resins; the amount of unbound protein in solution was determined by measuring the A_{280} absorbance of the supernatant, and the amount of protein bound by each resin was calculated via mass balance. (C) RYSPPPPYSSHS-Toyopearl (PTCH peptide, positive control) and Toyopearl HW65-F (negative control) resins were also incubated with WW-YAP protein (1 mg/mL). In panels (B) and (C), the mass of WW-YAP protein bound by each resin was normalized to the mass of WW-YAP protein bound by RYSPPPPYSSHS-Toyopearl (PTCH peptide) resin. Error bars correspond to the standard error of the mean from three independent replicates.

Following elution, the cDNA linked to the isolated mRNA-peptide fusions was amplified to generate a focused sub-library for subsequent screening rounds. We noted that, during the generation of the sub-libraries, heptamer and decamer sequences emerged. While potentially present as minor contaminants in the original library, these longer peptides may have outcompeted the original pentamers; the longer peptides likely benefit from a higher enthalpic contribution to their binding free energy due to the presence of more residues that can contact the target protein. Accordingly, the longer peptides were identified as lead fusions after multiple rounds of selection.

Sequencing returned 10 candidate WW-binding peptides: 3 pentamers, 2 heptamers, and 5 decamers (Figure 2A). Two of the returned pentamer sequences carried an overall positive charge while one sequence did not contain any charged residues. The returned pentamer sequences were mainly enriched in hydrophobic residues; One pentamer sequence contained a hydrophobic aromatic residue (WW.1). The returned heptamer sequences varied with one being enriched in basic residues while the other was enriched in acidic residues. Each heptamer sequence contained a variety of hydrophobic and polar residues. Of the decameric sequences, two were undetermined (i.e., Sanger sequencing returned unassigned residues "X"). The others contained a variety of hydrophobic and hydrophilic residues. Two decamer sequences have an overall negative charge, while another has an overall positive charged. Additionally, two decamer sequences contain hydrophobic aromatic residues (WW.6 and WW.10).

Due to the heterogeneity of the isolated sequences, only a few were evaluated further; Specifically, cyclo[M-AFRLC-K], cyclo[M-LDFVNHRSRG-K], cyclo[M-DGNLSGIMPV-K], and cyclo[M-YRGDPETCVD-K] were considered. Cyclic peptides containing larger sized rings will likely be able to contact a greater portion of the target protein, which may result in greater affinity. Therefore, we chose to focus our evaluation predominantly on the decamer sequences. A single pentamer sequence was also chosen to evaluate if smaller sized peptides can exhibit sufficient affinity. Specifically, cyclo[M-AFRLC-K] was selected as it contained the greatest diversity of residues among the pentamer sequences.

For evaluation, we performed equilibrium binding tests using peptide-functionalized resin and recombinant human WW-YAP (1 mg/mL). The cyclic peptides and their linear cognates were synthesized on solid phase (Toyopearl amino AF-650M) via standard Fmoc/tBu chemistry; Toyopearl resin functionalized with the known WW-binding peptide PTCH (RYSPPPPYSSHS)[19,20] and hydroxyl Toyopearl HW-65F

https://dx.doi.org/10.1021/acscombsci.0c00171
ACS Comb. Sci. 2020, 22, 738−744

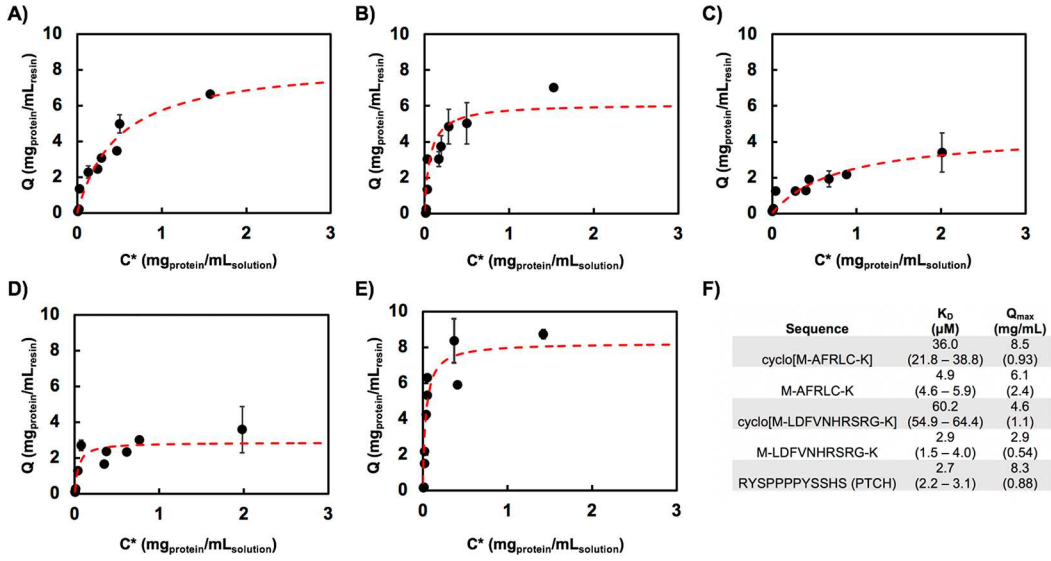

Sequence	K_D (μM)	Q_{max} (mg/mL)
cyclo[M-AFRLC-K]	36.0 (21.8 – 38.8)	8.5 (0.93)
M-AFRLC-K	4.9 (4.6 – 5.9)	6.1 (2.4)
cyclo[M-LDFVNHRSRG-K]	60.2 (54.9 – 64.4)	4.6 (1.1)
M-LDFVNHRSRG-K	2.9 (1.5 – 4.0)	2.9 (0.54)
RYSPPPPYSSHS (PTCH)	2.7 (2.2 – 3.1)	8.3 (0.88)

Figure 3. WW-YAP equilibrium binding isotherms for (A) cyclo[M-AFRLC-K]-Toyopearl, (B) MAFRCLK-Toyopearl, (C) cyclo[M-LDFVNHRSRG-K]-Toyopearl, (D) MLDFVNHRSRGK-Toyopearl, and (E) RYSPPPPYSSHS-Toyopearl (PTCH peptide) resins. The amount of protein bound to the resin (Q) is reported as a function of the concentration of protein in solution at equilibrium (C^*). Error bars represent the standard error of the mean for three independent experiments. (F) For C^* ranging from 20 μg/mL to 2 mg/mL of WW-YAP, a Langmuir isotherm model was fit to data globally to estimate a single value of K_D across the repeats and individual Q_{max} values (maximum protein binding capacity) for each repeat. In parentheses, a 68% confidence interval is provided for the K_D values while the standard deviation of the mean is provided for Q_{max}.

resin were adopted as positive and negative control adsorbents, respectively. Sequences AFRLC and LDFVNHRSRG showed significant WW-YAP binding, capturing 60% and 44% of the protein in solution in their cyclic form, and 68% and 60% in their linear form, respectively (Figure 2B); similarly, PTCH-Toyopearl resin bound >73% of the incubated WW-YAP (Figure 2C). In contrast, sequences DGNLSGIMPV and YRGDPETCVD showed poor WW-YAP binding and were discarded. It is not surprising that AFRLC and LDFVNHRSRG bound WW-YAP readily as these peptide sequences exhibit an overall positive charge and the isoelectric point of WW-YAP is around 4.88 (sequence predicted). Both DGNLSGIMPV and YRGDPETCVD, which did not bind WW-YAP, exhibit an overall negative charge. A negative selection against non-target displaying yeast was included in every round to eliminate binders to non-specific yeast surface proteins. Hence, it is likely that DGNLSGIMPV and YRGDPETCVD do have weak affinity for WW-YAP. However, the concentration of WW-YAP used in the resin studies may have been too low to observe binding or any bound WW-YAP may have been removed during washing. Such weak affinity binders likely would be eliminated after performing additional rounds of selection with greater stringency.

Positively interacting sequences, AFRLC and LDFVNHRSRG, were then characterized via adsorption isotherm studies to evaluate their binding strength and capacity. The assays were performed by incubating WW-YAP at varying concentrations (0.02−12.5 mg/mL) with cyclo[M-AFRLC-K]-Toyopearl, MAFRCLK-Toyopearl, cyclo[M-LDFVNHRSRG-K]-Toyopearl, MLDFVNHRSRGK-Toyopearl, and RYSPPPPYSSHS -Toyopearl (PTCH peptide) resins. The values of adsorbed protein (Q, mass of WW-YAP bound per mL of resin) vs equilibrium concentration in solution (C^*, mass of WW-YAP per mL of solution) were fit using model isotherms. The isotherms and corresponding values of binding capacity (Q_{max}) and affinity (K_D) are presented in Figure 3. In all cases, a Langmuir−Freundlich behavior was observed, wherein a Langmuir-only profile is observed at $C^* < 2$ mg/mL, and the Freundlich profile becomes dominant at $C^* > 2$ mg/mL (Figure S2). It was noted that the linear form of the selected sequences possess a higher affinity for WW-YAP than their corresponding cyclic form; while cyclic peptides generally feature higher affinity compared to their linear counterparts, instances have been reported of linear peptides with higher protein-targeting activity.[21] It is possible that AFRLC and LDFVNHRSRG were selected in their linear form during the selections if cyclization was incomplete during library synthesis. However, the majority of the mRNA-peptide hybrids are likely cyclized as suggested by previous reverse phase HPLC analysis. In that study, cyclic peptides of similar length were cyclized using a similar cross-linking chemistry at a yield greater than 87%.[6]

Asymptotic Langmuir behavior plateauing above C^* of 2 mg/mL was replaced by linear increasing Freundlich behavior (Figure S2), which may be the result of WW-YAP protein aggregation. WW domains are structured as a bundle of three antiparallel β-sheets.[22] As the concentration in solution increases, free WW-YAP can self-assemble onto the initial cohort of peptide-bound WW, thereby promoting the formation of an aggregated layer. As the WW-YAP: WW-YAP interaction is likely weaker than the WW-YAP: peptide affinity bond, the binding isotherms exhibit a Freundlich profile at higher concentrations, where significant WW-YAP adsorption occurs due to aggregation. Figure S2 showcases the binding isotherms combining Langmuir and Freundlich profiles, while Table S1 reports the resulting binding parameters, including binding affinity (K_D), maximum binding capacity (Q_{max}), distribution coefficient (K), and correction factor (n).

Finally, we evaluated the use of cyclo[M-AFRLC-K]-Toyopearl and cyclo[M-LDFVNHRSRG-K]-Toyopearl resins as adsorbents for protein purification in bind-and-elute mode (Table S2). Notably, complete recovery of bound WW-YAP was achieved using a low-pH glycine buffer. This demonstrates

https://dx.doi.org/10.1021/acscombsci.0c00171
ACS Comb. Sci. 2020, 22, 738−744

the utility of these identified cyclic peptides as potential purification ligands.

It was surprising that a linear form of a peptide exhibited a higher affinity than its cyclic counterpart. Therefore, we investigated the binding strength and orientation of peptides MAFRCLK-GSG, cyclo[M-AFRLC-K]-GSG, MLDFVNHRSRGK-GSG, cyclo[M-LDFVNHRSRG-K]-GSG, and RYSPPPPYSSHS-GSG (PTCH peptide) *in silico* using molecular docking. The peptide models, initially generated using molecular dynamics (MD), were docked against the crystal structure of WW-YAP (PDB ID: 2LTW) using HADDOCK (High Ambiguity Driven Protein-Protein Docking, v.2.2).[23] A GSG (Gly-Ser-Gly) spacer located on the C-terminus of the peptides was marked as "inactive" to ensure its outward orientation within the WW:peptide complexes; the GSG spacer is utilized to link the peptides on the Toyopearl resin and is not involved in binding. The resulting clusters for each WW:peptide complex were ranked using the scoring functions FireDock and XScore,[24] and the top binding poses were subsequently evaluated by atomistic MD simulations to estimate the free energy of binding (ΔG_B). Representative examples of modeled WW:peptide complexes are reported, and the values of K_D calculated from the averaged values of binding energy (ΔG_B) are listed (Figure 4). The docking results indicate that the peptides identified from our screens bind to WW-YAP in a similar region as the SMAD7 (GESPPPPYSRYPMD, PDB ID: 2LTW)[25] and PTCH peptides,[19] both of which feature the known WW-binding PPXY motif (X: any guest amino acid). The calculated values

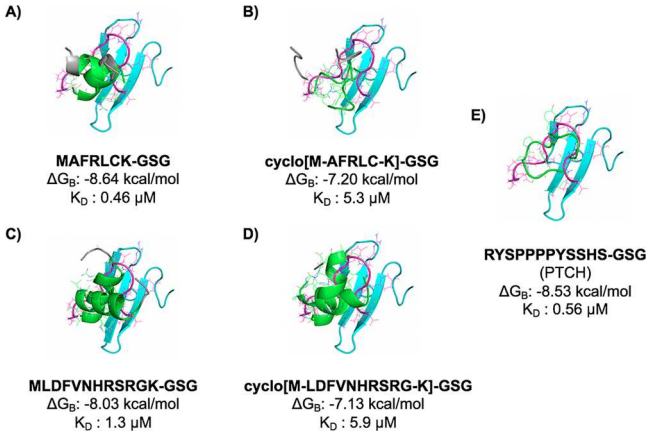

Figure 4. *In silico* WW:peptide complexes obtained by molecular docking and refined by molecular dynamics simulation for (A) MAFRLCK-GSG, (B) cyclo[M-AFRLC-K]-GSG, (C) MLDFVNHRSRGK, (D) cyclo[M-LDFVNHRSRG-K]-GSG, and (E) RYSPPPPYSSHS-GSG (PTCH peptide). WW-YAP is denoted in cyan, while the peptides discovered in this work are designated in green with their GSG segment in gray and the SMAD7 peptide in magenta. The values of binding energy (ΔG_B) and corresponding affinity (K_D) of the WW:peptide complexes derived from the docking and MD simulations are noted. The binding energy and affinity estimates for the WW:PTCH peptide complex as predicted by molecular simulation are similar to values previously predicted using isothermal titration calorimetry, −6.24 kcal/mol and 27.6 μM, respectively.[19] The interaction of SMAD7, a WW-binding peptide, was also evaluated using molecular docking and MD simulation (*in silico* complex alone not shown). The binding energy and binding affinity of the WW:SMAD7 complex were estimated as −8.2 kcal/mol and 0.99 μM, respectively.

of K_D are in good agreement with those estimated from the equilibrium adsorption studies, especially in that the linear peptides bind WW-YAP stronger than their cyclic counterparts. The slightly higher affinity predicted by the MD simulations compared to the results of the binding isotherms can be attributed to the non-ideality of the binding events on the chromatographic resin. *In silico*, the WW-YAP target and the peptide ligand enjoy complete rotational freedom and lack of topological constraints, except for defining GSG as a passive linker. In contrast, the binding on the chromatographic resin is influenced by the roughness of the surface and the orientation of the peptides conjugated on it.

The mRNA-display selection process was repeated to identify affinity peptides for another target protein, TOM22. After five rounds of selection, ten individual colonies were sequenced and seven complete sequences were returned (Figure 5A). The majority of these sequences exhibit an

A)

	M	X_1	X_2	X_3	X_4	X_5	X_6	X_7	X_8	X_9	X_{10}	K
TOM22.1		S	V	H	L	R						
TOM22.2		G	V	H	R	N						
TOM22.3		R	G	Q	A	R	A	Y				
TOM22.4		P	E	L	N	R	A	I				
TOM22.5		R	C	S	H	A	L	G	A	R	E	
TOM22.6		T	V	K	D	R	F	C	R	M	F	
TOM22.7		L	Q	A	E	G	G	D	M	W	M	

B)

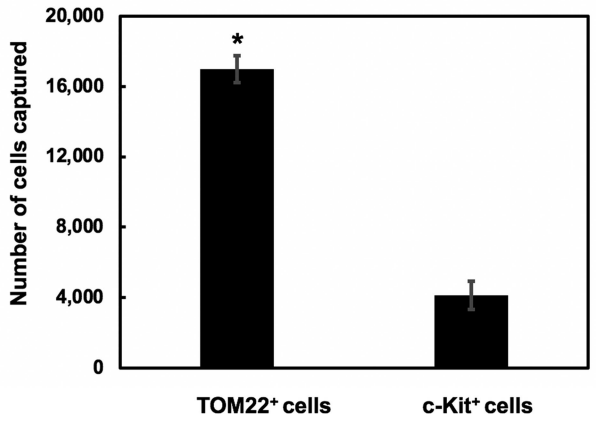

Figure 5. Identified TOM22-binding cyclic peptides and specificity characterization. (A) Amino acid sequences of peptides isolated from the selection of a mRNA-display cyclic peptide library against yeast-displayed TOM22. (B) Recovery of yeast cells displaying TOM22 or c-Kit by magnetic beads functionalized with cyclo[M-PELNRAI-K]. Yeast cells expressing TOM22 or c-Kit also displayed an engineered luciferase protein as a yeast surface fusion. Cell capture was quantified as a function of the luminescence signal produced by the recovered population using a generated luminescence standard curve. * represents $p < 0.05$ for a two-tailed, paired t test in comparison to the recovery of c-Kit displaying yeast cells.

overall positive charge, which likely promotes interaction with negatively charged TOM22 (isoelectric point ~4).[26] Only two of the isolated sequences exhibit either a neutral or negative overall charge, TOM22.4 and TOM22.7, respectively. The anionic character of TOM22 is instrumental for protein translocation across mitochondria, as translocating proteins contain positively charged pre-sequences. Previous studies identified a TOM22-binding peptide, KTGALLLQ,[27] which is

https://dx.doi.org/10.1021/acscombsci.0c00171
ACS Comb. Sci. 2020, 22, 738−744

cationic and rich in hydrophobic residues, like the sequences identified in our selection. Another TOM22-binding sequence identified in the same study, LCTKVPEL, contains one cationic residue and one anionic residue, and a balance of hydrophobic and hydrophilic amino acids, similar to cyclo[M-PELNRAI-K] identified in this work. Based on the diversity of these previously identified TOM22-binding peptides, it is not surprising that we also isolated a diverse set of peptides from our screens.

We resolved to study the TOM22 binding of cyclo[M-PELNRAI-K]. The chemical diversity of this peptide, which contains positively (R) and negatively charged (E), polar (N), and hydrophobic (A, I, L, and P) residues, is conducive to TOM22-binding by true affinity. Briefly, yeast cells co-expressing TOM22 and luciferase were incubated with magnetic beads functionalized with cyclo[M-PELNRAI-K] in the presence of non-displaying EBY100 yeast cells, which were included to reduce non-specific binding. Yeast cells bound to the peptide-functionalized beads were isolated using a magnet and subjected to a luminescence-based assay, wherein the luminescence signal is proportional to the number of TOM22-displaying cells captured by the magnetic beads. A study by Bacon et al. describes how this assay can be used to quantitatively rank ligands with different affinities for a target protein;[28] the correlation between the number of TOM22-displaying cells and luminescence signal is reported in a calibration curve detailed in Figure S3.

We also considered the binding of cells co-displaying a non-target protein (c-Kit) and luciferase to magnetic beads functionalized with peptide cyclo[M-PELNRAI-K]. We observed that TOM22$^+$ yeast cells were captured by the peptide-functionalized beads at a statistically (∼4.5-fold) higher level than TOM22$^-$/c-KIT$^+$ cells (Figure 5B), suggesting that cyclo[M-PELNRAI-K] is selective for TOM22. Based on the capture levels of the TOM22$^+$ cells by the magnetic peptide beads, in comparison to other protein interactions studied previously using this luciferase assay, it is likely that the binding strength of the TOM22:cyclo[M-PELNRAI-K] complex is rather moderate.[28] Nonetheless, the described luminescence-based assay was capable of detecting mild interactions owing to the multi-point binding mechanism (avidity) between cells and the peptide-functionalized beads as well as the inherent sensitivity of the luciferase reporter. Due to its low affinity, we did not evaluate this peptide in the context of targeted delivery to mitochondria.

Taken together, we demonstrated isolation of cyclic peptide affinity ligands for two protein targets—WW-YAP and TOM22—by combinatorial screening of mRNA-display libraries using magnetic yeast displaying the target proteins. Values of protein-binding affinity in the μM range, as those measured in this work, are typical for linear and cyclic peptides of 6−10 amino acids in length.[29] It is however possible to enhance the affinity of peptide ligands selected combinatorially to reach a low-μM/high-nM range by adjusting the sequence length of the protein-binding segment to increase the enthalpic component of the binding energy.[29] Care should be taken in adjusting the protein-binding segment of cyclic peptides to prevent excessive flexibility of the peptide backbone, which would unfavorably affect the entropic component of the binding energy. The library screening process can also be revisited to improve the binding affinity of isolated mutants by increasing the stringency of the selections. In this work, the selection conditions were maintained throughout the successive screening rounds, and only the elution conditions were adjusted; alternatively, competitive conditions can be adopted when incubating the library with the target cells by adding a mixture of soluble competitors, or by adjusting the composition, concentration, and pH of the selection buffer. Additional wash steps can also be performed to eliminate weak-affinity binders. Further, while held constant in this work, the number of protein-displaying cells could be reduced through the successive screening rounds to bias the isolation of higher affinity mutants. Finally, a larger number of selection rounds, beyond the four or five employed here, up to 10, can be performed to attain strong sequence homology among the identified peptides;[30] nonetheless, this work has shown that specific binding peptides can be identified using fewer rounds of screening.

Collectively, our results show that the use of magnetic yeast displaying a target protein is an effective tool to increase the throughput of library screening. Our approach limits the need for recombinant soluble protein and provides an alternative approach for screening mRNA-display libraries. The use of yeast-displayed targets will be most effective for proteins that do not require complex post-translational modifications for their function, since glycosylation patterns may vary between yeast and other higher order eukaryotes.

EXPERIMENTAL PROCEDURES

Details on experimental procedures used in this study can be found in the Supporting Information.

ASSOCIATED CONTENT

Supporting Information

The Supporting Information is available free of charge at https://pubs.acs.org/doi/10.1021/acscombsci.0c00171.

Experimental methods; Figure S1, WW-YAP and TOM22 yeast surface expression; Figure S2, WW-YAP equilibrium Langmuir−Freundlich binding isotherms; Figure S3, luminescence calibration curves; Table S1, values predicted from WW-YAP equilibrium Langmuir−Freundlich binding isotherms; Table S2, values from WW-YAP bind-and-elute studies; Table S3, oligonucleotide primers; Table S4, gene block fragments; and Table S5, peptide oligonucleotides (PDF)

AUTHOR INFORMATION

Corresponding Authors

Balaji M. Rao − *Department of Chemical and Biomolecular Engineering and Biomanufacturing Training and Education Center (BTEC), North Carolina State University, Raleigh, North Carolina 27606, United States;* orcid.org/0000-0001-5695-8953; Email: bmrao@ncsu.edu

Stefano Menegatti − *Department of Chemical and Biomolecular Engineering and Biomanufacturing Training and Education Center (BTEC), North Carolina State University, Raleigh, North Carolina 27606, United States;* orcid.org/0000-0001-5633-434X; Email: smenega@ncsu.edu

Authors

Kaitlyn Bacon − *Department of Chemical and Biomolecular Engineering, North Carolina State University, Raleigh, North Carolina 27606, United States*

https://dx.doi.org/10.1021/acscombsci.0c00171
ACS Comb. Sci. 2020, 22, 738−744

John Bowen − *Department of Chemical and Biomolecular Engineering, North Carolina State University, Raleigh, North Carolina 27606, United States*

Hannah Reese − *Department of Chemical and Biomolecular Engineering, North Carolina State University, Raleigh, North Carolina 27606, United States*

Complete contact information is available at: https://pubs.acs.org/10.1021/acscombsci.0c00171

Author Contributions

[§]K.B. and J.B. contributed equally.

Notes

The authors declare no competing financial interest.

■ ACKNOWLEDGMENTS

This work was funded by three grants from the National Science Foundation (CBET 1511227, CBET 1510845, and CBET 1743404). K.B. and H.R. kindly acknowledge support from an NSF Graduate Research Fellowship. K.B. and J.B. kindly acknowledge support from a National Institutes of Health Molecular Biotechnology Training Fellowship (NIH T32). We would also like to thank the UNC High-Throughput Peptide Synthesis and Array facility for peptide synthesis.

■ REFERENCES

(1) Galán, A.; Comor, L.; Horvatić, A.; Kuleš, J.; Guillemin, N.; Mrljak, V.; Bhide, M. Library-Based Display Technologies: Where Do We Stand? *Mol. BioSyst.* **2016**, *12* (8), 2342−2358.

(2) Roberts, R. W.; Szostak, J. W. RNA-Peptide Fusions for the in Vitro Selection of Peptides and Proteins. *Proc. Natl. Acad. Sci. U. S. A.* **1997**, *94* (23), 12297−12302.

(3) Wang, H.; Liu, R. Advantages of MRNA Display Selections over Other Selection Techniques for Investigation of Protein-Protein Interactions. *Expert Rev. Proteomics* **2011**, *8*, 335−346.

(4) Wójcik, P.; Berlicki, Ł. Peptide-Based Inhibitors of Protein-Protein Interactions. *Bioorg. Med. Chem. Lett.* **2016**, *26* (3), 707−713.

(5) Davies, J. S. The Cyclization of Peptides and Depsipeptides. *J. Pept. Sci.* **2003**, *9* (8), 471−501.

(6) Menegatti, S.; Hussain, M.; Naik, A. D.; Carbonell, R. G.; Rao, B. M. MRNA Display Selection and Solid-Phase Synthesis of Fc-Binding Cyclic Peptide Affinity Ligands. *Biotechnol. Bioeng.* **2013**, *110* (3), 857−870.

(7) Bacon, K.; Burroughs, M.; Blain, A.; Menegatti, S.; Rao, B. M. Screening Yeast Display Libraries against Magnetized Yeast Cell Targets Enables Efficient Isolation of Membrane Protein Binders. *ACS Comb. Sci.* **2019**, *21* (12), 817−832.

(8) Vieira Gomes, A.; Souza Carmo, T.; Silva Carvalho, L.; Mendonça Bahia, F.; Parachin, N. Comparison of Yeasts as Hosts for Recombinant Protein Production. *Microorganisms* **2018**, *6* (2), 38.

(9) Zhao, L.; Qu, L.; Zhou, J.; Sun, Z.; Zou, H.; Chen, Y.-Y.; Marks, J. D.; Zhou, Y. High Throughput Identification of Monoclonal Antibodies to Membrane Bound and Secreted Proteins Using Yeast and Phage Display. *PLoS One* **2014**, *9* (10), No. e111339.

(10) Safarik, I.; Maderova, Z.; Pospiskova, K.; Baldikova, E.; Horska, K.; Safarikova, M. Magnetically Responsive Yeast Cells: Methods of Preparation and Applications. *Yeast* **2015**, *32* (1), 227−237.

(11) Schwegmann, H.; Feitz, A. J.; Frimmel, F. H. Influence of the Zeta Potential on the Sorption and Toxicity of Iron Oxide Nanoparticles on S. Cerevisiae and E. Coli. *J. Colloid Interface Sci.* **2010**, *347* (1), 43−48.

(12) Gera, N.; Hussain, M.; Rao, B. M. Protein Selection Using Yeast Surface Display. *Methods* **2013**, *60* (1), 15−26.

(13) Kieke, M. C.; Shusta, E. V.; Boder, E. T.; Teyton, L.; Wittrup, K. D.; Kranz, D. M. Selection of Functional T Cell Receptor Mutants from a Yeast Surface-Display Library. *Proc. Natl. Acad. Sci. U. S. A.* **1999**, *96* (10), 5651−5656.

(14) Piccolo, S.; Dupont, S.; Cordenonsi, M. The Biology of YAP/TAZ: Hippo Signaling and Beyond. *Physiol. Rev.* **2014**, *94* (4), 1287−1312.

(15) van Wilpe, S.; Ryan, M. T.; Hill, K.; Maarse, A. C.; Meisinger, C.; Brix, J.; Dekker, P. J. T.; Moczko, M.; Wagner, R.; Meijer, M.; et al. Tom22 Is a Multifunctional Organizer of the Mitochondrial Preprotein Translocase. *Nature* **1999**, *401* (6752), 485−489.

(16) Kang, Y. C.; Son, M.; Kang, S.; Im, S.; Piao, Y.; Lim, K. S.; Song, M.; Park, K.; Kim, Y.; Pak, Y. K. Cell-Penetrating Artificial Mitochondria- Targeting Peptide-Conjugated Metallothionein 1A Alleviates Mitochondrial Damage in Parkinson's Disease Models. *Exp. Mol. Med.* **2018**, *50* (8), 105.

(17) Boder, E. T.; Wittrup, K. D. Yeast Surface Display for Screening Combinatorial Polypeptide Libraries. *Nat. Biotechnol.* **1997**, *15* (6), 553−557.

(18) Millward, S. W.; Fiacco, S.; Austin, R. J.; Roberts, R. W. Design of Cyclic Peptides That Bind Protein Surfaces with Antibody-like Affinity. *ACS Chem. Biol.* **2007**, *2* (9), 625−634.

(19) Iglesias-Bexiga, M.; Castillo, F.; Cobos, E. S.; Oka, T.; Sudol, M.; Luque, I. WW Domains of the Yes-Kinase-Associated-Protein (YAP) Transcriptional Regulator Behave as Independent Units with Different Binding Preferences for PPxY Motif-Containing Ligands. *PLoS One* **2015**, *10* (1), No. e0113828.

(20) Schuchardt, B. J.; Mikles, D. C.; Hoang, L. M.; Bhat, V.; McDonald, C. B.; Sudol, M.; Farooq, A. Ligand Binding to WW Tandem Domains of YAP2 Transcriptional Regulator Is under Negative Cooperativity. *FEBS J.* **2014**, *281* (24), 5532−5551.

(21) Roxin, Á.; Zheng, G. Flexible or Fixed: A Comparative Review of Linear and Cyclic Cancer-Targeting Peptides. *Future Med. Chem.* **2012**, *4* (12), 1601−1618.

(22) Macias, M. J.; Hyvönen, M.; Baraldi, E.; Schultz, J.; Sudol, M.; Saraste, M.; Oschkinat, H. Structure of the WW Domain of a Kinase-Associated Protein Complexed with a Proline-Rich Peptide. *Nature* **1996**, *382* (6592), 646−649.

(23) Van Zundert, G. C. P.; Rodrigues, J. P. G. L. M.; Trellet, M.; Schmitz, C.; Kastritis, P. L.; Karaca, E.; Melquiond, A. S. J.; Van Dijk, M.; De Vries, S. J.; Bonvin, A. M. J. J. The HADDOCK2.2 Web Server: User-Friendly Integrative Modeling of Biomolecular Complexes. *J. Mol. Biol.* **2016**, *428* (4), 720−725.

(24) Spiliotopoulos, D.; Kastritis, P. L.; Melquiond, A. S. J.; Bonvin, A. M. J. J.; Musco, G.; Rocchia, W.; Spitaleri, A. dMM-PBSA: A New HADDOCK Scoring Function for Protein-Peptide Docking. *Front. Mol. Biosci.* **2016**, *3*, 46.

(25) Aragón, E.; Goerner, N.; Xi, Q.; Gomes, T.; Gao, S.; Massagué, J.; MacIas, M. J. Structural Basis for the Versatile Interactions of Smad7 with Regulator WW Domains in TGF-β Pathways. *Structure* **2012**, *20* (10), 1726−1736.

(26) Yano, M.; Hoogenraad, N.; Terada, K.; Mori, M. Identification and Functional Analysis of Human Tom22 for Protein Import into Mitochondria. *Mol. Cell. Biol.* **2000**, *20* (19), 7205−7213.

(27) Bellot, G.; Cartron, P.-F.; Er, E.; Oliver, L.; Juin, P.; Armstrong, L. C.; Bornstein, P.; Mihara, K.; Manon, S.; Vallette, F. M. TOM22, a Core Component of the Mitochondria Outer Membrane Protein Translocation Pore, Is a Mitochondrial Receptor for the Proapoptotic Protein Bax. *Cell Death Differ.* **2007**, *14* (4), 785−794.

(28) Bacon, K.; Blain, A.; Bowen, J.; Burroughs, M.; McArthur, N.; Menegatti, S.; Rao, B. M. Quantitative Yeast-Yeast Two Hybrid for Discovery and Binding Affinity Estimation of Protein-Protein Interactions. *bioRxiv Preprint* **2020**, 247874.

(29) Tavassoli, A. SICLOPPS Cyclic Peptide Libraries in Drug Discovery. *Curr. Opin. Chem. Biol.* **2017**, *38*, 30−35.

(30) Guillen Schlippe, Y. V.; Hartman, M. C. T.; Josephson, K.; Szostak, J. W. In Vitro Selection of Highly Modified Cyclic Peptides That Act as Tight Binding Inhibitors. *J. Am. Chem. Soc.* **2012**, *134* (25), 10469−10477.